Basic sciences

Nuclear Medicine Review 2006
Vol. 9, No. 1, pp. 6–11

ISSN 1506–9680

VIA MEDICA

# Small animal imaging using a conventional gamma camera exemplified in studies on the striatal dopaminergic system

Christoph Scherfler[1], Clemens Decristoforo[2]

[1]Department of Neurology, Department of Nuclear Medicine, Innsbruck Medical University, Austria
[2]Department of Nuclear Medicine, Innsbruck Medical University, Austria

[Received 20 XII 2005; Accepted 28 XII 2005]

## Abstract

BACKGROUND: Small animal imaging has recently been the subject of increasing interest and specific imaging devices in particular for positron emission tomography (PET) have been developed. To bypass limitations arising from high acquisition costs and dependence on an in-house cyclotron unit inevitably associated with PET, a conventional gamma camera has been equipped with a pinhole collimator and used to visualize striatal pre- and post-synaptic dopaminergic function in rats measured by the dopamine transporter ligand [$^{123}$I]$\beta$-CIT and the dopamine D2/ dopamine D3 receptor ligand [$^{123}$I]IBZM. In order to precisely estimate brain regions of low radioligand uptake, single photon emission computed tomography (SPECT) images were coregistered onto an MRI template.
MATERIAL AND METHODS: Our pinhole SPECT/MRI approach has been employed in animal models of pre- and postsynaptic dopaminergic dysfunction. The physical characteristics of the scanner, the tracer kinetics and modelling as well as image postprocessing have been addressed and associated intrinsic problems and constraints discussed.
CONCLUSIONS: An outlook has been provided on the application of pinhole SPECT and MRI coregistration towards non-invasive investigations of drug-receptor interactions and binding characteristics of newly developed radiopharmaceuticals.
**Key words: pinhole SPECT, MRI, coregistration, dopamine transporter, dopamine D2/D3 receptor, striatum**

*Correspondence to:* Clemens Decristoforo
Department of Nuclear Medicine, Innsbruck, Medical University
Anichstrasse 35, A-6020 Innsbruck, Austria
Tel: (+43) 512 504 80951; fax (+43) 512 504 25498
e-mail: clemens.decristoforo@uibk.ac.at

## Introduction

Advances in image resolution and sensitivity of dedicated small animal positron emission tomographs (PET) and single photon emission computed tomographs (SPECT) are attracting increasing interest in basic sciences [1]. Radioligands with selective binding properties and PET enable the visualization of biochemical processes in the animal's brain, give clues on the binding characteristics of newly developed radiopharmaceuticals and facilitate the characterization of disease processes in animals over time. As a non-invasive tool, animals may be repeatedly subjected to PET, allowing for serial study designs and consequently reducing the number of animals needed. Apart from optical imaging approaches [2] nuclear medicine techniques are of specific interest as they provide information of molecular processes in cells and the functional status of tissues (molecular and functional imaging).

However, dedicated devices for small animal PET and SPECT are associated with high investments and hence are not widely available. In particular, PET is closely linked to an on-site cyclotron enabling the supply of radionuclides in sufficient amounts. To circumvent the lack of availability of those devices, we have equipped a conventional single headed gamma camera with a pinhole collimator, resulting in a three to four fold increase in spatial resolution. In order to estimate precisely areas of low radioligand uptake, SPECT images were coregistered onto MRI sequences obtained by a conventional whole body 1.5 Tesla scan-

ner. Following characterization of spatial resolution, system sensitivity and accuracy of SPECT-MRI coregistration the system was challenged to characterize the striatal pre-and postsynaptic dopaminergic function in a living rat [3, 4]. Information of the presynaptic dopaminergic function in the rat striatum was obtained by 2-$\beta$--carbomethoxy-3-$\beta$-(4-[$^{123}$I]iodophenyl) tropane ([$^{123}$I]$\beta$-CIT), a cocaine derivative with high affinity for the dopamine transporter (DAT). Postsynaptic striatal dopamine D2/D3 receptor (D2/D3R) availability was assessed by the radioligand [$^{123}$I] iodobenzamide ([$^{123}$I] IBZM). We describe the properties of the system and its use in the evaluation of animals with normal and impaired striatal dopaminergic function. Correlations with ex-vivo markers of the pre- and postsynaptic dopaminergic system have been performed.

This paper recounts our experiences which are more widely applicable to small animal radiotracer imaging, and examines some of the experimental settings where such techniques are most likely to make a significant contribution. Finally, the future potential will be explored in the light of new technological developments.

## Characterization of our SPECT system

SPECT data were acquired using a rotating single-headed gamma camera (Siemens Orbiter ZLC 3700) equipped with a pinhole collimator and a 2.0 mm aperture insert. Data acquisition was performed over a circular orbit of 360° (64 projections; 60 s/projection); acquisition matrix size was 128 × 128 pixels, with 16 bit depth. For [$^{123}$I]IBZM pinhole SPECT acquisitions were performed 81 min post-tracer injection (p.i.), and for [$^{123}$I]$\beta$-CIT 320 min p.i. Studies were acquired using a 15% energy window, centred on the 159 keV photopeak of [$^{123}$I]. Due to the magnification of the pinhole collimator, a separate correction of the centre of rotation shift was necessary. SPECT images were reconstructed by means of filtered backprojection based on a cone-beam algorithm (Nuclear Diagnostics, Sweden). As a prefilter, a Butterworth filter was applied with an order of 5 and a cutoff frequency of 0.4 cycles cm$^{-1}$. No corrections for attenuation and scatter were performed. Anatomical information of the rat brain was obtained with the help of a modified whole body 1.5-T MRI scanner (Siemens) equipped with a flex loop. The MRI protocol included a T2-weighted spine echo sequence (TR, 3000 ms; TE, 96 ms; matrix 256 × × 256 pixels, slice thickness 2 mm; field of view (FoV) 65 mm; acquisition time ~13 min). In order to precisely define regions of interest (ROIs) on the SPECT images, the individual SPECT data set was transferred on a previously computed MRI template, averaging three individual MRIs of normal rats. The fully automated registration approach is based on the maximization of mutual information [5] and implemented into SPM 99 (Statistical Parametric Mapping, Wellcome Dept. Cogn. Neurol., London) [6]. ROIs were then drawn on related anatomical structures visualized on the MRI template and transposed to the corresponding SPECT slice using the MRIcro software (version 1.37, Chris Rorden, Nottingham, UK).

System sensitivity, spatial resolution, and SPECT-MRI coregistration measurements were obtained using different phantoms at a radius of 45mm from the pinhole collimator aperture to the axis of the collimator rotation. Studies of the dependence of system resolution on the radius of rotation have been reported by Weber and colleagues [7]. System sensitivity was 0.081 cps/kBq for a 2.0 mm aperture pinhole collimator. The measured reconstructed axial and transaxial in-plane resolution calculated as full width at half maximum (FWHM) was 3.5 mm including the effects of applied filters. The average misregistration between MRI and SPECT images as measured by the distance between external markers on both image modalities was 1.2 mm in the transaxial plane and 1.1 mm in the axial plane.

## Pinhole SPECT imaging of striatal dopaminergic function in the rat

Prior to assess radiotracer uptake in animals with dopaminergic dysfunction the optimal injection dose and acquisition period have to be determined in healthy animals. Male Wistar rats with narrow weights ranging from 290g to 310g were scanned serially over seven hours at different tracer dosages. Washout rates (%/h) of the striatum and cerebellum have been calculated and the data fitted to a model accordingly (please see section: Tracer kinetics and modelling). Once the optimal tracer dose and acquisition period was determined, striatal [$^{123}$I]$\beta$-CIT and [$^{123}$I]IBZM binding was assessed in animal models of pre- and postsynaptic dopaminergic dysfunction. To mimic the decrease of DAT availability, which is related to the loss of dopaminergic neurons, the well-established and frequently cited 6-hydroxydopamine (6-OHDA) model of Parkinson's disease (PD) was used [8]. 6-OHDA, a synthetic neurotoxin has been reported by Ungerstedt to selectively destroy dopaminergic neurons projecting from the substantia nigra to the striatum when injected into the medial forebrain bundle of the rat [9]. Five animals received 8 $\mu$l 6-OHDA (2 $\mu$g/$\mu$l) into the left medial forebrain bundle [10]. The striatal [$^{123}$I]$\beta$-CIT uptake has been correlated to surviving dopaminergic neurons in the substantia nigra visualized by tyrosinhydroxylase immunohistochemistry. Linear regression analysis showed that the measurements of striatal [$^{123}$I]$\beta$-CIT uptake and nigral tyrosinhydroxylase positive cell counts were highly correlated, confirming the sensitivity of [$^{123}$I]$\beta$-CIT pinhole SPECT for assessing dopaminergic deficits in lesioned animals. This is in line with a small animal pinhole SPECT study in unilaterally dopamine depleted mice showing tight correlations of striatal DAT binding and ex vivo DAT immunohistochemistry [11].

Analogous to 6-OHDA lesioning of the medial forebrain bundle, postsynaptic decline of striatal D2/D3R expression was achieved by administering the N-methyl-D-aspartate receptor agonist quinolinic acid (QA) stereotactically into the striatum, well-known as a rat model of Huntington's disease [12]. QA induces selective neuronal degeneration of D2/D3R baring medium-sized spiny neurons, which are known to express the dopamine and cyclic adenosine 3'5'-monophosphate-regulated phosphorus-protein (DARPP-32) in high concentrations. DARPP-32 positive neurons can be visualized by immunohistochemistry. In our model high correlations between striatal IBZM uptake values and both volume and optical density measures of remaining striatum were found in animals of increasing striatal D2/D3R damage. Correlations between striatal lesions and motor tasks performed in those animals were weaker when compared to striatal IBZM uptake, suggesting in particular in animals with small striatal lesions that IBZM pinhole SPECT is more sensitive in the detection of mild striatal dopaminergic dysfunction.

## Practical issues in pinhole SPECT imaging of small animals

### *Animal positioning and injection of the radioligand*

Imaging artefacts caused by head movements or motion caused by breathing must be kept to a minimum as those will lead to a positional shift severely affecting SPECT-MRI coregistration. To keep animals motionless the use of anaesthetics is strongly suggested. The choice of anaesthetic agent relies on its binding characteristics to neuroreceptors and must not interfere with the radiotracer administered [13]. At our department isoflurane anaesthesia is used routinely as this is not reported to interact with the dopaminergic system. In case of new radioligands, cross validation with other anaesthetics are recommended using ex-vivo methods for receptor quantification. Once the rat is anaesthetized a femoral vein can be easily canulated for bolus injection or continuous infusion of the radioligand and then placed to the tomograph. To guarantee accurate positioning of the animal in the FoV and to facilitate SPECT-MRI coregistration the rat's head has been held in a Perspex stereotaxic frame (based on the commercial Kopf small--animal stereotaxic frame), which keeps artefacts caused by gamma ray and nuclear magnetic resonance to a minimum.

### *Small animal gamma cameras*

Recently a number of dedicated devices for small animal SPECT imaging have been described. Del Guerra et al reported on an integrated PET-SPECT system based on four detector heads with $4 \times 4 \times 4$cm $YAlO_3$: Ce crystals [14]. In this system a comparable resolution with slightly higher sensitivity is achieved (3.1 mm FWHM and 0.031cps/kBq).

Another system is based on the use of multiple pinhole SPECT and conventional gamma camera technologies. By applying a dedicated iterative reconstruction software, high resolution images can be acquired. By using such a device, termed NanoSPECT (Bioscan, Washington DC, USA) a spatial resolution below 1 mm FWHM and sensitivity of 1cps/kBq can be achieved. Similarly high resolution has been reported from another system based a slit-parallel rake collimation (Linoview Systems BV, Amsterdam, the Netherlands). Although these systems now offer imaging studies even in mice with high restrict sensitivity, considerable acquisition costs restricts its application to dedicated imaging research centres.

### *Specification of radioligands*

[$^{123}$I]IBZM was obtained from Amersham Health B.V. (Eindhoven, the Netherlands) with a radiochemical purity of 95% and a specific activity > 74 GBq/$\mu$mol. [$^{123}$I]$\beta$-CIT has been delivered from the Arsenal Research (Seibersdorf, Austria) with a radiochemical purity >95% and specific activity > 55 GBq/$\mu$mol. The count statistics per voxel in the striatum at equilibrium conditions was highest in animals receiving 37MBq ([$^{123}$I]$\beta$-CIT) and 44.4MBq ([$^{123}$I]IBZM) and comparable to voxel values in humans. Our data support previous reports, indicating that high resolution imaging of small animals cannot be performed with tracer doses scaled down to ratios of animal to human body masses [15, 16]. The reason for this is that the size of the resolution "voxel" appropriate to the rat scales with the mass to the animal. A rat is about 230 times smaller in mass and size compared to a human. The volume of a voxel in our animal study is 1 mm$^3$ whereas in a human SPECT acquisition it is about 64 mm$^3$. To gain the same statistical precision of measured activity in the voxels of a rat, at least a quarter to one-third of the radioactivity administered to a human must then be delivered to the small animal voxels assuming comparable system sensitivities of the human and small animal SPECT study. However, injections of nearly equivalent amounts of radioligand as compared to humans might elicit a pharmacological response and in addition violate the assumptions underlying tracer kinetic models. It is generally believed that a receptor occupancy of 5% represents the threshold at which the dose can no longer be considered as a tracer quantity and may elicit a pharmacological response. Based on receptor occupancy studies for raclopride, a D2/D3 agonist with comparable receptor affinity, the maximum injectable dose of 74 MBq was calculated for [$^{123}$I]IBZM, respectively. Considering tolerable bolus injection maxima in rats of 0.5–1 ml without endangering the animal's blood circulation, we set the maximum of our bolus injection volume to 0.7 ml and this resulted in activities of 44.4 MBq and 37 MBq for [$^{123}$I]IBZM and [$^{123}$I]$\beta$-CIT, respectively. Generally the evaluation of potential mass effects in small animal imaging is crucial, especially when studying low capacity targets such as receptors [17].

### *Tracer kinetics and modelling*

In order to derive adequate measures tracer kinetics have been assessed for [$^{123}$I]$\beta$-CIT and [$^{123}$I]IBZM by serial scans. True tracer equilibrium conditions requiring tracer washout rates below 5%/h were identified for [$^{123}$I]$\beta$-CIT from 285-355min p.i. As a consequence the equilibrium model for [$^{123}$I]$\beta$-CIT reported by Laruelle and colleagues was applied to our datasets since it does not require multiple scans or the measurement of arterial plasma tracer concentration [18]. The outcome measure, which is termed specific-to-nondisplaceable equilibrium partition coefficient ($V_3$"), is proportional to the ratio of receptor density ($B_{max}$). The equilibrium model relies on several assumptions: first, the stability of regional tracer uptake during image acquisition, and second, the negligible DAT receptor density in the cerebellum representing the non--specific bound and free activity.

Serial scans following a bolus of [$^{123}$I]IBZM identified washout rates of more than 5%/h in the striatum and cerebellum; however, the slopes of tracer uptake in the striatum and cerebellum were identical from 81–355 min p.i. indicating a secular equilibrium, which is known to be a constant linear function of ratios obtained at true equilibrium again providing an index of $B_{max}$ [19].

### *Magnetic resonance imaging coregistration and ROI analysis*

Since D2/D3R and DAT-SPECT does not provide anatomical details of brain areas with nonspecific radioligand uptake such as the cerebellum or occipital cortex and of specific tracer uptake such as the dopamine and D2/D3R-depleted striatum from surrounding areas, anatomical information of those ROIs is needed. To guarantee fully automated processing of imaging data ranging from data acquisition to the calculation of regional count statistics, an image coregistration approach based on mutual information, a basic concept from information theory, described by Collignon and co-workers, was successfully introduced for SPECT--MRI coregistration in our studies [5]. Brain templates consisting

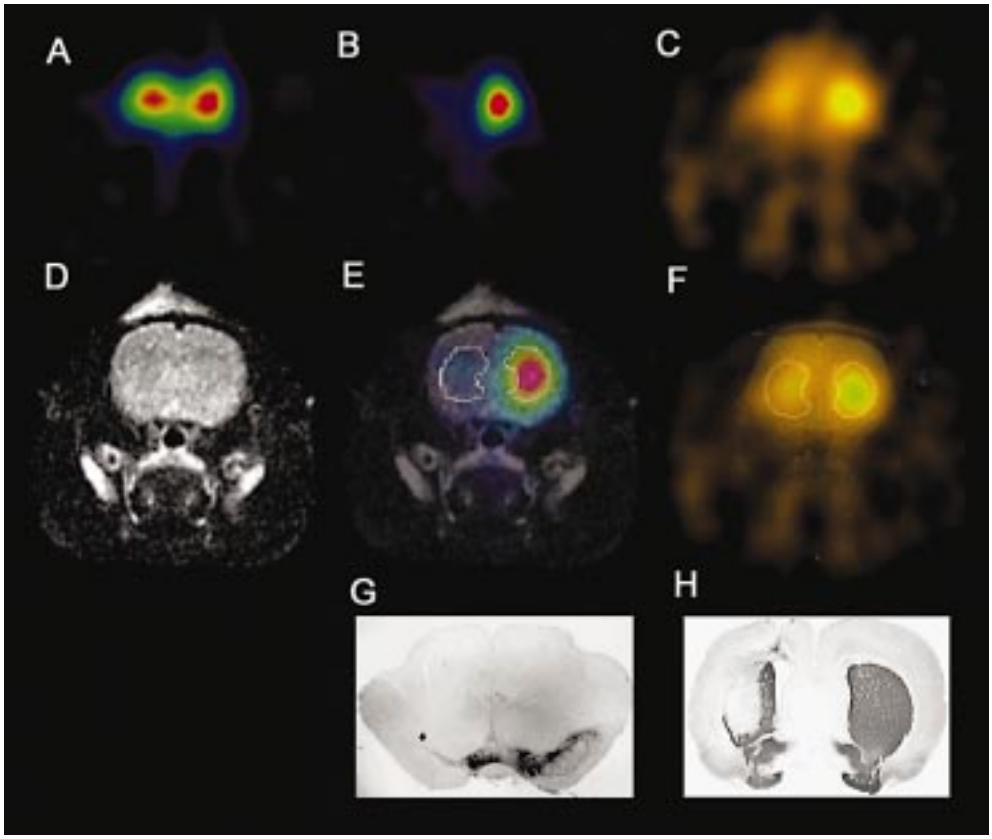


**Figure 1.** Selected examples of pinhole SPECT using a conventional gamma camera system (Siemens Orbiter). **A.** Coronal sections of striatal uptake of $^{123}$I-$\beta$-CIT in a normal rat; **B.** Unilaterally 6-OHDA lesioned rat; **D.** The corresponding MR slice; **E.** [$^{123}$]$\beta$-CIT SPECT image coregistered onto the corresponding MRI slice; **G.** The ex vivo immunohistochemical staining of dopaminergic neurons in the substantia nigra; **C.** [$^{123}$I]IBZM pinhole SPECT of the striatum of a unilaterally QA lesioned rat, again coregistered onto the corresponding MRI slice (**F**); **H**. Ex vivo DARPP-32 immunohistochemistry of striatal neurons in the same animal.

of healthy rats were built for [$^{123}$I]IBZM/[$^{123}$I]$\beta$-CIT SPECT and T2 weighted MRI. Consecutively, SPECT templates have been coregistered onto the MRI template. Since the decline of count statistics and associated structural resolution in lesioned animals limited the application of aligning the SPECT image directly onto the MRI, the individual SPECT image was matched to the corresponding SPECT template previously coregistered onto the MRI template. Finally, ROIs have been delineated on the MRI template and transposed onto the individual SPECT image (Figure 1).

## Applications of pinhole SPECT imaging

### *Characterization of animal models based on neuroreceptor dysfunction*

The in-vivo assessment of animal models of Parkinson's disease and Huntington's disease primarily relnies on behavioural tests sensitive to striatal dopaminergic dysfunction [20–22]. Behavioural tests, although economic and simple, often fail to accurately reflect mild to moderate degrees of striatal dopaminergic dysfunction [23]. In contrast small animal PET and 18F-DOPA and [$^{11}$C] raclopride enable direct insights into the striatal dopaminergic system [24]. The feasibility to visualize striatal DAT and D2/D3R distributions in rats and mice and its correlation with behavioural parameters has also been reported for small animal pinhole SPECT [3, 4, 7, 25, 26]. It has to be pointed out that improvement of spatial resolution by pinhole collimators is achieved at the expense of reduced counts per voxel. Lower system sensitivity, however is compensated in part by the utilization of tracers labelled with longer half-life isotopes as [$^{123}$I] and [$^{99m}$Tc], characterized by very high specific activities, which are at least equivalent or higher than those achieved with conventional PET radionuclides. Typical examples of pinhole SPECT in normal and unilaterally lesioned rats using both $^{123}$I-IBZM as well as $^{123}$I-$\beta$-CIT are shown in Figure 1. Coregistration with MRI allows anatomical localisation and ex vivo immunohistochemistry shows good correlation with tracer uptake in lesioned animals. The gamma camera setup is shown in Figure 2.

When reviewing the literature, the characterization of the striatal dopaminergic system in small animals with PET and SPECT has attracted the most attention of researchers. To a minor extent reports on the application of [$^{99m}$Tc]-HMPAO to visualize blood perfusion of small brain structures or brain tumours are available [7, 27]. Ohmori and colleagues investigated the lipid metabolism in a middle cerebral artery occlusion model with pinhole SPECT using an [$^{123}$I]labelled diacylglycerol [28]. Pinhole SPECT was also shown to be useful in visualizing with [$^{123}$I] iomazenil the distribution of GABA-A receptors in the brains of rats [27]. The use

Nuclear Medicine Review 2006, Vol. 9, No. 1

**Figure 2.** Pinhole-SPECT setup as used in this study employing conventional single headed gamma camera (Siemens Orbiter) equipped with a 2 mm pinhole aperture.

of pinhole SPECT for the characterization of animal models of cerebral diseases is still in its infancy and further studies with radioligands evaluating cerebral blood perfusion and metabolism in rodents are needed to extend its application to numerous animal models in the fields of cerebro-vascular and neurodegenerative diseases as well as epilepsy.

## Characterization of radioligands

Animal SPECT is increasingly applied towards evaluation of new radiopharmaceuticals. The advantage over classical dissection and gamma counting lies in the fact that the number of animals necessary can be reduced and pharmacokinetic behaviour such as excretion patterns, organ uptake and tissue retention over time can be visualized. This becomes increasingly important in the development of radiotracers for brain imaging [29], but also for other applications such as oncology [30, 31]. Some challenges may be addressed by using SPECT, for others (e.g., excretion patterns) dynamic planar imaging might be sufficient.

## Characterization of drug-receptor interactions

Another interesting approach might be to study receptor occupancy by novel drugs, evaluated with specifically designed radiotracers with high affinity and selectivity for these target binding sites. Occupancy of D2Rs in the mouse striatum has been measured for cold raclopride with the SPECT tracer [123I] IBF under tracer-to-receptor equilibrium conditions using constant infusion techniques [32]. This setting allows the kinetics of drugs acting on the same receptor to be modelled.

Of course, a special advantage is the option of subsequent imaging of the same animal e.g. before and after drug treatment, giving better insight into regulatory effects potentially caused by the compound to be tested on the neuroreceptor expression. Those studies are of particular interest when pursuing the discussion on potential long term effects of initial dopamine agonist administration versus levodopa in early PD. A 46-month follow up assessment revealed a significant one-third reduction in relative rates of decline of striatal [$^{123}$I]$\beta$-CIT uptake in the dopamine agonist arm compared with the levodopa arm [33]. The possibility that dopamine agonists and levodopa itself might exert regulatory influences to various degrees on the number of DAT expressed, the radiotracer affinity and receptor occupancy led to major difficulties in the interpretation of the clinical relevance of such findings [34, 35] and suggests that this issue needs to be addressed prior to the application of DAT SPECT as a biomarker for the effects of dopaminergic treatment on the nigrostriatal dopaminergic system.

## Conclusion

The system described herein allows the use of a conventional SPECT system, available in every nuclear medicine department, to be used for high resolution imaging of small animals. Potential fields of application of pinhole SPECT and MRI coregistration are seen in the characterization of animal models, the non-invasive and repetitive investigations of drug-receptor interactions and evaluation of biodistribution and binding characteristics of newly developed radiopharmaceuticals.

## Acknowledgments

This work was supported by the Austrian Federal Ministry of Education, Science and Culture (BM BWK GZ 70038). We wish to thank GE Healthcare Austria for providing [$^{123}$I]-IBZM.

Part of this work was presented at the 12$^{th}$ European Symposium on Radiopharmacy and Radiopharmaceuticals in Gdansk, Poland.

## References

1. Herschman HR. Molecular imaging: looking at problems, seeing solutions. Science 2003; 302: 605–608.
2. Choy G, Choyke P, Libutti SK. Current advances in molecular imaging: noninvasive in vivo bioluminescent and fluorescent optical imaging in cancer research. Mol Imag 2003; 2: 303–312.
3. Scherfler C, Donnemiller E, Schocke M et al. Evaluation of striatal dopamine transporter function in rats by in vivo beta-[123I]CIT pinhole SPECT. Neuroimage 2002; 17: 128–141.
4. Scherfler C, Scholz SW, Donnemiller E et al. Evaluation of [123I]IBZM pinhole SPECT for the detection of striatal dopamine D2 receptor availability in rats. Neuroimage 2005; 24: 822–831.
5. Collignon A, Maes F, Delaere D, Vandermeulen D, Suetens P, Marchal G. Automated multi-modality image registration based on information theory. In: The proceedings of information processing in medical imaging. Bizais Y (ed). Kluwer Academic, New York 1995: 263–274.
6. Friston K, Ashburner J, Poline JB, Frith CD, Heather JB, Frackowiak RSJ. Spatial registration and normalization of images. Hum Brain Mapp 1995; 2: 165–189.
7. Weber DA, Ivanovic M, Franceschi et al. Pinhole SPECT: an approach to in vivo high resolution SPECT imaging in small laboratory animals. J Nucl Med 1994; 35: 342–348.
8. Schwarting RKW and Huston JP. Unilateral 6-Hydroxydopamine lesions of meso-striatal dopamine neurons and their physiological sequelae. Progr Neurobiol 1996; 49: 215–266.

9. Ungerstedt U. 6-Hydroxy-dopamine induced degeneration of central momamine neurons. Eur J Pharmacol 1968; 5: 107–110.
10. Blunt SB, Jenner P, Marsden CD. Autoradiographic study of striatal D1 and D2 dopamine receptors in 6-OHDA-lesioned rats receiving foetal ventral mesencephalic grafts and chronic treatment with L-dopa and carbidopa. Brain Res 1992; 582: 299–311.
11. Andringa G, Drukarch B, Bol JG et al. Pinhole SPECT imaging of dopamine transporters correlates with dopamine transporter immunohistochemical analysis in the MPTP mouse model of Parkinson's disease. Neuroimage 2005; 15: 1150–1158.
12. Beal MF, Kowall NW, Ellison DW, Mazurek MF, Swartz KJ, Martin JB. Replication of the neurochemical characteristics of Huntington's disease by quinolinic acid. Nature 1986; 321: 168–171.
13. Myers R. The biological application of small animal PET imaging. Nucl Med Biol 2001; 28: 585–593.
14. Del Guerra A, Damiani C, Di Domenico G, Scandola M, Zavattini G. High spatial resolution small animal imager: preliminary results. IEEE Trans Nucl Sci 2000; 47: 1537–1540.
15. Green MV, Seidel J, Vaquero JJ, Jagoda E, Lee I, Eckelman WC. High resolution PET, and projection imaging in small animals. Comput Med Imag Graph 2001; 25:79–86.
16. Acton PD, Kung HF. Small animal imaging with high resolution single photon emission tomography. Nucl Med Biol 2003; 30: 889–895.
17. Kung MP, Kung HF. Mass effect of injected dose in small rodent imaging by SPECT and PET. Nucl Med Biol 2005; 32: 673–678.
18. Laruelle M, Wallace E, Seibyl JP et al. Graphical, kinetic, and equilibrium analyses of in vivo [123I] beta-CIT binding to dopamine transporters in healthy human subjects. J Cereb Blood Flow Metab 1994; 14: 982–994.
19. Carson RE, Channing MA, Blasberg RG, et al. Comparison of bolus and infusion methods for receptor quantitation: application to [18F]cyclofoxy and positron emission tomography. J Cereb Blood Flow Metab 1993;13: 24–42.
20. Schwarcz R, Whetsell WO, Mangano RM. Quinolinic acid — an endogenous metabolite that produces axon-sparing lesions in rat brain. Science 1983; 219: 316–318.
21. Montoya CP, Astell CP, Dunnett SB. Effects of nigral and striatal grafts on skilled forelimb use in the rat. Prog Brain Res 1990; 82: 459–466.
22. Fricker RA, Annett LE, Torres EM, Dunnett SB. The Placement of a striatal ibotenic acid lesion affects skilled forelimb use and the direction of drug-induced rotation. Brain Res Bull 1996; 41: 409–416.
23. Dunnett SB, Iversen SD. Spontaneous and drug-induced rotation following localised 6-hydroxydopamine and kainic acid-induced lesions of the neostriatum. Neuropharmacol 1982; 21: 899–908.
24. Hume SP, Lammertsma AA, Myers R et al. The potential of high-resolution positron emission tomography to monitor striatal dopaminergic function in rat models of disease. J Neuroscien Meth 1996; 67: 103–112.
25. Habraken JB, de Bruin K, Shehata M et al. Evaluation of high-resolution pinhole SPECT using a small rotating animal. J Nucl Med 2001; 42: 1863–1869.
26. Acton PD, Choi SR, Plossl K, Kung HF. Quantification of dopamine transporters in the mouse brain using ultra-high resolution single-photon emission tomography. Eur J Nucl Med 2002a; 29: 691–698.
27. Ishizu K, Mukai T, Yonekura Y et al. Ultra-high resolution SPECT system using four pinhole collimators for small animal studies. J Nucl Med 1995; 36: 2287–2289.
28. Ohmori Y, Imahori Y, Ueda S et al. Radioiodinated diacylglycerol analogue: a potential imaging agent for single-photon emission tomographic investigations of cerebral ischaemia. Eur J Nucl Med 1996; 23: 280–289.
29. Pimlott SL. Radiotracer development in psychiatry. Nucl Med Commun 2005; 26: 183–188.
30. Schurrat T, Alfke H, Behe M et al. Molecular gastrin receptor localisation in mice using high-resolution SPET-MRI image fusion. Eur J Nucl Med Mol Imaging 2003; 30: 800.
31. Haubner RH, Wester HJ, Weber WA, Schwaiger M. Radiotracer-based strategies to image angiogenesis. Q J Nucl Med 2003; 47: 189–199.
32. Acton PD, Hou C, Kung MP, Plossl K, Keeney CL, Kung HF. Occupancy of dopamine D2 receptors in the mouse brain measured using ultra-high-resolution single-photon emission tomography and [123I]IBF. Eur J Nucl Med 2002; 29: 1507–1515.
33. Parkinson Study Group. Pramipexole vs levodopa as initial treatment for Parkinson disease: A randomized controlled trial. Parkinson Study Group. JAMA 2000; 284: 1931–1938.
34. Ahlskog JE. Slowing Parkinson's disease progression: recent dopamine agonist trials. Neurology 2003; 60: 381–389.
35. Wooten GF. Agonists vs. levodopa in PD: the thrilla of whitha. Neurology 2003; 60: 360 –362.